

Engineered bacteria can function in the mammalian gut long-term as live diagnostics of inflammation

David T Riglar^{1,2}, Tobias W Giessen^{1,2}, Michael Baym^{1,3} , S Jordan Kerns^{1,2,6}, Matthew J Niederhuber^{1,2}, Roderick T Bronson⁴, Jonathan W Kotula^{1,2,6}, Georg K Gerber⁵ , Jeffrey C Way² & Pamela A Silver^{1,2}

Bacteria can be engineered to function as diagnostics or therapeutics in the mammalian gut but commercial translation of technologies to accomplish this has been hindered by the susceptibility of synthetic genetic circuits to mutation and unpredictable function during extended gut colonization. Here, we report stable, engineered bacterial strains that maintain their function for 6 months in the mouse gut. We engineered a commensal murine *Escherichia coli* strain to detect tetrathionate, which is produced during inflammation. Using our engineered diagnostic strain, which retains memory of exposure in the gut for analysis by fecal testing, we detected tetrathionate in both infection-induced and genetic mouse models of inflammation over 6 months. The synthetic genetic circuits in the engineered strain were genetically stable and functioned as intended over time. The durable performance of these strains confirms the potential of engineered bacteria as living diagnostics.

Bacteria in the gut microbiome can sense, respond to and manipulate the mammalian gut environment. Recombinant probiotics that have been engineered to exploit these features show promise as therapeutics and diagnostics for inflammatory bowel disease (IBD), autoimmune diabetes, obesity and other conditions¹. However, engineered, live bacterial diagnostics and therapies have been tested only under non-colonizing conditions in the guts of model organisms and humans. Furthermore, engineered bacteria for other applications such as tumor-targeted strains of *Salmonella enterica* serovar Typhimurium (hereafter referred to as *Salmonella typhimurium*) are cleared from the body within ~1 month in mouse and non-human primate models². If recombinant probiotic bacterial strains could colonize the mammalian gut and function for extended periods, the potential for translation of such technologies to humans would be vastly improved¹. Unfortunately, the burden that synthetic genetic circuits place on their bacterial hosts³ can result in compensatory genetic mutations⁴, loss of engineered function⁵ or lack of growth of the recombinant strain³ in a host- and environment-dependent manner^{6,7}.

Live, engineered bacteria can be used as non-invasive diagnostics to detect transient (or highly localized) molecules in the gut, or as thera-

peutics. The gut environment is largely inaccessible, and products of digestion or those released by the host or microbiome can be modified by the microbiome, or absorbed by the host, before excretion. Several bacterial strains have been engineered to detect transient gene expression in the laboratory^{8–11} and *in vivo* for up to 12 d^{12,13}. We previously engineered *E. coli* to record exposure to tetracycline and its analogs¹². Our engineered strain contained two circuits, an environmentally responsive promoter driving Cro protein expression, which functioned as a ‘trigger’, and a Cro-inducible CI/Cro transcriptional switch derived from phage lambda, which functioned as a ‘memory element’¹². The engineered *E. coli* detected anhydrotetracycline in the mouse gut and retained memory of this for up to 7 d following removal of the signal. However, the engineered strain responded to tetracycline derivatives, which might alter the microbiome through toxicity, thereby preventing meaningful long-term analysis of strain stability and function in a physiologically relevant environment.

Here, we report the design of a trigger circuit that can detect and respond to tetrathionate. Tetrathionate is a transient product of reactive oxygen species (ROS), which are produced during inflammation¹⁴. Our aim was to develop a strain that could detect this inflammatory marker and study the ability of the strain to colonize and function in the murine gut over an extended time period.

The conversion of thiosulfate, which is produced from hydrogen sulfide, into tetrathionate in the mouse intestine has been reported during inflammation induced by *S. typhimurium*¹⁴ and *Yersinia enterocolitica*¹⁵ (**Supplementary Fig. 1**). Tetrathionate is detected in these bacteria by the TtrR/TtrS two-component system¹⁶ and can be used as a terminal electron acceptor for anaerobic respiration, providing a growth advantage to these pathogens during inflammation^{14,15,17,18}. A range of other bacteria, including pathogens, may also be able to grow preferentially using tetrathionate¹⁹. Increased production of tetrathionate in mice deficient in toll-like receptor-1 (ref. 15) and an enrichment of tetrathionate utilization genes in the microbiota of a *Tbet^{-/-}Rag^{-/-}* mouse ulcerative colitis (TRUC) model²⁰ point to the potential of tetrathionate as a general marker of inflammation. However, non-invasive detection of tetrathionate is not possible, which has limited further investigation.

¹Department of Systems Biology, Harvard Medical School, Boston, Massachusetts, USA. ²Wyss Institute for Biologically Inspired Engineering, Harvard University, Boston, Massachusetts, USA. ³Department of Biomedical Informatics, Harvard Medical School, Boston, Massachusetts, USA. ⁴Department of Microbiology and Immunology, Harvard Medical School, Boston, Massachusetts, USA. ⁵Massachusetts Host-Microbiome Center, Department of Pathology, Brigham and Women's Hospital, Harvard Medical School, Boston, Massachusetts, USA. ⁶Present addresses: Emulate Inc., Boston, Massachusetts, USA (S.J.K.) and SynLogic, Cambridge, Massachusetts, USA (J.W.K.). Correspondence should be addressed to P.A.S. (pamela_silver@hms.harvard.edu).

Received 20 September 2016; accepted 7 April 2017; published online 29 May 2017; doi:10.1038/nbt.3879

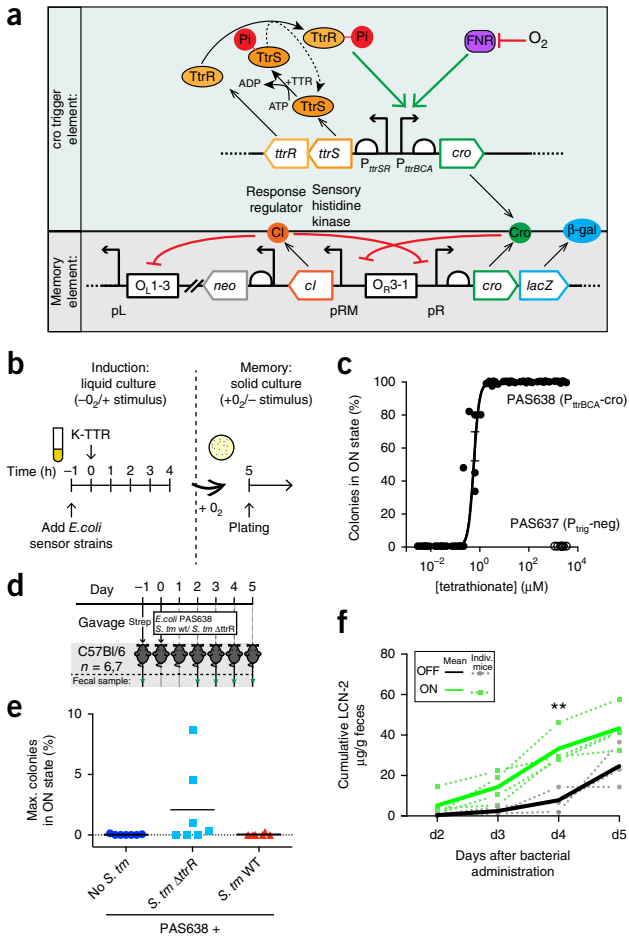


Figure 1 Engineering a tetrathionate-responsive memory device in *E. coli* NGF-1. **(a)** A bacterial memory device, PAS638, was constructed in mouse commensal *E. coli* NGF-1. *S. typhimurium* *ttrR/S* and P_{ttrBCA} drive Cro ‘trigger’ expression to switch a phage-lambda-based memory circuit¹². In the presence of tetrathionate, TtrS becomes phosphorylated, in turn phosphorylating TtrR, which activates expression through P_{ttrBCA} in anaerobic conditions. Cro protein expression switches memory ON, accompanied by *lacZ* reporter expression. **(b)** Testing of *in vitro* memory. **(c)** A dose–response curve of PAS638 (EC_{50} : 0.38–0.85 μM ; 95% CI) but no response of the triggerless control PAS637 strain. Graph shows individual values from six replicate colonies from two separate experiments, nonlinear fit \pm s.e.m. **(d)** PAS638 and *S. typhimurium* 14028s (*S. tm*) bacteria were administered by oral gavage to mice one day after streptomycin treatment, and fecal samples were analyzed days 2–5 after administration. Green star: fecal sample collected. **(e)** Specific response of PAS638 on day 4 and/or 5 when co-infected with *S. typhimurium* $\Delta ttrR$ bacteria ($n = 7$) but not control ($n = 7$) or *S. typhimurium* WT bacteria ($n = 6$). **(f)** Cumulative LCN-2 levels in mice administered PAS638 plus *S. typhimurium* $\Delta ttrR$ were higher in mice with PAS638 response (green lines) than in those without (black lines). Graph shows plots for individual mice (dotted) and ON or OFF averages (solid lines). ** t -ratio(5) = 4.3, $P = 0.03$ using multiple Student’s t -tests with Holm–Sidak multiple comparisons test, and each time point analyzed individually without assuming a consistent s.d. Day (d)2 (t -ratio(5) = 1.2, $P = 0.3$), d3 (t -ratio(5) = 2.5, $P = 0.1$) and d5 (t -ratio(5) = 2.3, $P = 0.1$) were not significantly different.

We engineered the commensal mouse *E. coli* strain NGF-1 to detect tetrathionate (Fig. 1a). Briefly, we constructed a trigger element using *ttrR/S* genes and the P_{ttrBCA} promoter from *S. typhimurium* to drive Cro expression, and inserted it into the genome of strain PAS637,

already containing our previously published memory circuit¹², thereby creating *E. coli* strain PAS638 (Fig. 1a and Supplementary Table 1). All synthetic constructs were integrated into the chromosome of *E. coli* strain NGF-1 to reduce burden and allow long-term circuit retention without selection. Engineered strain PAS638 exhibits ‘memory’ upon tetrathionate exposure, by driving Cro and β -galactosidase (β -gal) expression from the synthetic memory element and maintaining their expression in the absence of tetrathionate. We induced memory during anaerobic growth in liquid culture by adding tetrathionate, which should activate expression through P_{ttrBCA} in the trigger element and switch the memory element from the off (CI^+/Cro and β -gal⁻) to the on (Cro and β -gal⁺/ CI^-) state (Fig. 1b). We quantified the response of the circuit by plating tetrathionate-activated cultures onto solid media containing 5-bromo-4-chloro-3-indolyl- β -D-galactopyranoside (X-gal), which turns blue in the presence of β -gal. Plating in the absence of tetrathionate and under aerobic conditions allowed optimal maturation of the X-gal indicator plates as well as ensuring only colonies retaining a record of tetrathionate exposure were counted (Fig. 1b). PAS638 bacteria were effectively induced by tetrathionate (EC_{50} : 0.38–0.85 μM ; 95% CI), whereas the control strain, PAS637 (Supplementary Table 1), which does not contain the P_{ttrBCA} -cro trigger, showed no on/off switching even at saturating concentrations of 2 mM tetrathionate (Fig. 1c).

Having validated that PAS638 could record tetrathionate exposure *in vitro*, we next tested the ability of PAS638 to detect tetrathionate *in vivo* using a murine *S. typhimurium*-induced colitis model²¹ (Fig. 1d). The presence of inflammation, specifically ROS, causes elevated levels of tetrathionate that are rapidly reduced to thiosulfate by wild-type *S. typhimurium* strains, but not by strains deficient in tetrathionate-reduction capacity¹⁴. We pre-treated C57Bl/6 mice with streptomycin to reduce colonization resistance for *S. typhimurium* in the colon, and introduced by oral gavage PAS638, PAS638 with *S. typhimurium* or PAS638 with a *S. typhimurium* $\Delta ttrR$ variant that is unable to express tetrathionate reductase (Fig. 1d and Supplementary Table 1)¹⁸. Fecal samples were collected at days 2–5 after bacterial administration. PAS638 did not switch on β -gal expression in control and *S. typhimurium*-infected mice (Fig. 1e). However, when PAS638 was co-administered with *S. typhimurium* $\Delta ttrR$, switching was increased, with 4/7 mice showing a higher proportion of memory-on colonies than any samples from control mice on days 4–5 post-infection (Fig. 1e and Supplementary Fig. 2a). Colony forming unit (CFU) counts for PAS638 *E. coli* (Supplementary Fig. 2b) and *S. typhimurium* variants (Supplementary Fig. 2c) were generally consistent between groups and showed no correlation with switching. We hypothesized that the mice in which PAS638 was switched on should also show signs of more acute inflammation.

We independently validated the presence of inflammation in the colitis model using quantification of the lipocalin-2 (LCN-2) biomarker (Supplementary Fig. 2d)²² and blinded histopathology scoring of cecum and colon sections (Supplementary Fig. 2e,f). Taken together these techniques identified inflammation in all mice infected with *S. typhimurium* or *S. typhimurium* $\Delta ttrR$ ¹⁴. Of note, mice infected with *S. typhimurium* $\Delta ttrR$ in which memory-on state PAS638 colonies were detected had significantly ($P = 0.03$) higher cumulative LCN-2 values at day 4 post-infection than those in which PAS638 remained off (Fig. 1f). These results show that our engineered memory strain specifically senses tetrathionate and that tetrathionate sensing corresponds to a more acute inflammatory response *in vivo*.

Next, we set out to use PAS638 to further probe the pathways required for tetrathionate production. The Cytochrome B-245 Beta Chain gene (*cybb*; also known as *gp91phox* and *Nox2*), which encodes

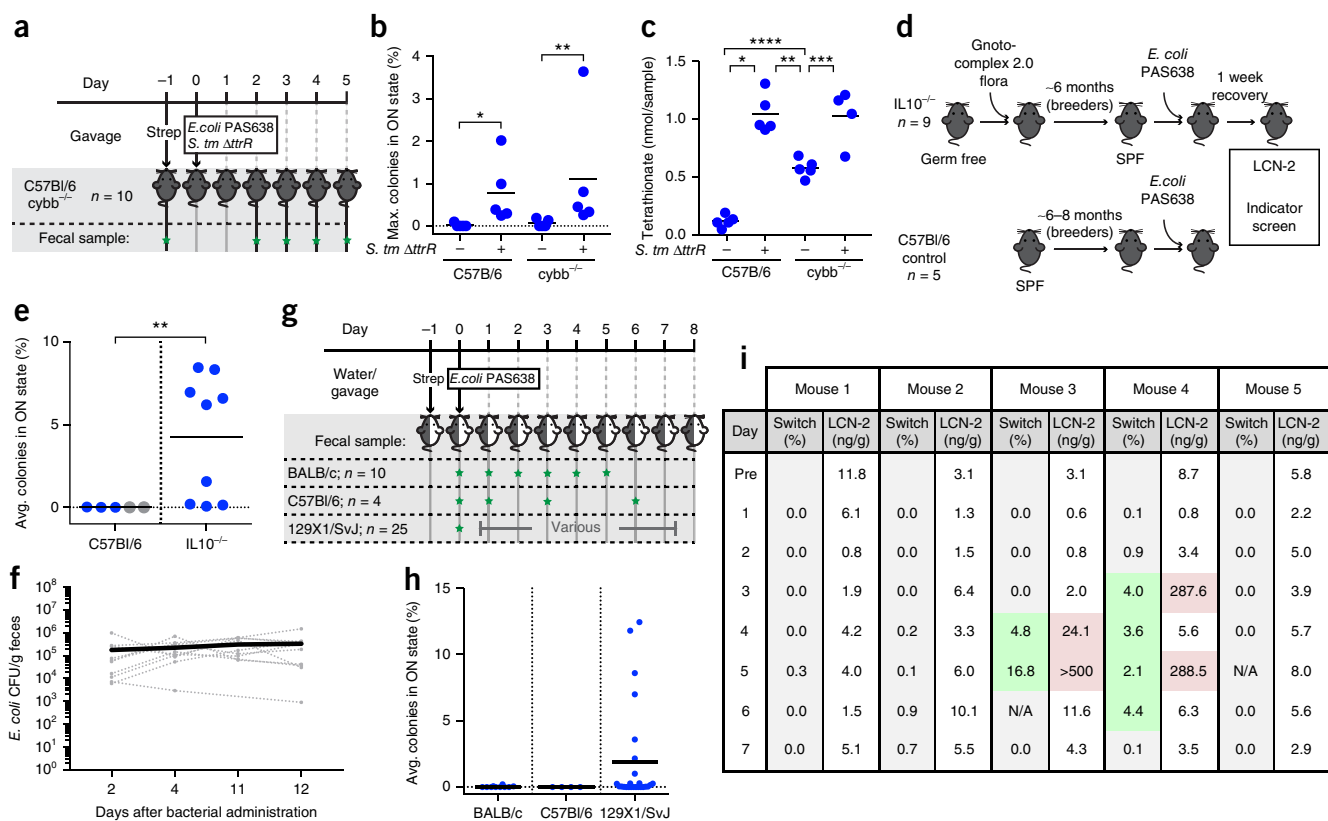


Figure 2 Tetrathionate-sensing of inflammation *in vivo*. (a) PAS638 and *S. typhimurium* $\Delta ttrR$ bacteria were administered to *cybb*^{-/-} and C57Bl/6 control mice ($n = 5$ per group) by oral gavage a day after streptomycin treatment. Green star: fecal sample collected. (b) Elevated PAS638 switching in the presence of *S. typhimurium* $\Delta ttrR$ indicated the presence of tetrathionate in both strains. Graph shows maximum percentage ON colonies over 5-d experiment; means are marked by horizontal lines. $*P = 0.01$ and $**P = 0.03$ using Kruskal-Wallis test with Dunn's multiple comparison correction. A comparison between the two *S. tm* $\Delta ttrR$ samples was also done, $P > 0.99$. (c) Mass spectrometry from cecal extracts confirmed that tetrathionate was raised in *cybb*^{-/-} and C57Bl/6 mice co-infected with *S. typhimurium* $\Delta ttrR$, along with intermediate levels in *cybb*^{-/-} uninfected controls. Graph shows total tetrathionate detected per whole cecum; means are marked. $*P < 0.0001$, $**P = 0.0008$, $***P = 0.002$ and $****P = 0.0009$; $F(3, 15) = 42.92$ using one-way ANOVA with Tukey's multiple comparison correction. Comparison of both infected groups ($P = 0.996$) and C57Bl/6 control with *cybb*^{-/-} infected mice ($P < 0.0001$) were performed but are not shown. (d) PAS638 was administered to retired breeder IL10^{-/-} mice raised in gnotobiotic and barrier specific-pathogen-free (SPF) conditions and to retired breeder C57Bl/6 control mice raised in SPF conditions. (e) Indicator plating of fecal samples from C57Bl/6 and IL10^{-/-} mice (>1 week after administration) showed elevated tetrathionate response in IL10^{-/-} mice. Blue, average of 3–4 measurements from individual mice. Gray, single measurement from individual mice. Means are marked with horizontal lines. $**P = 0.009$ between groups (including only blue values) using a two-tailed Mann-Whitney test. (f) PAS638 stably colonized IL10^{-/-} mice ($n = 10$), even without streptomycin pre-treatment. Graph shows CFU counts for individual mice (dotted lines) and average of all mice (solid). (g) BALB/c, C57Bl/6 and 129X1/SvJ mice were colonized with PAS638 and the bacterial memory state was analyzed (green star: fecal sample collected). (h) BALB/c and C57Bl/6 mice showed no switching, while a subset of 129X1/SvJ mice showed elevated response. Graph shows averages from at >3 d for individual mice and means. (i) PAS638 levels broadly correlated with increased LCN-2 levels in five 129X1/SvJ mice. Time points in which bacteria were more highly switched into the memory-on state tended to correspond with higher LCN-2 levels. Memory values >1%, green; >20 ng/g, red.

a subunit of the phagocyte NADPH-oxidase complex, has previously been implicated in the generation of tetrathionate¹⁴. We tested the response of PAS638 to *S. typhimurium* $\Delta ttrR$ infection of *cybb*-deficient (*cybb*^{-/-}) mice (Fig. 2a). Unexpectedly, PAS638 showed increased switching specifically in *S. typhimurium* $\Delta ttrR$ -infected *cybb*^{-/-} mice (Fig. 2b). *S. typhimurium* $\Delta ttrR$ -infected *cybb*^{-/-} mice also had more acute weight loss and increased fecal LCN-2 levels compared with *S. typhimurium* $\Delta ttrR$ -infected C57Bl/6 controls (Supplementary Fig. 3a,b). Uninfected *cybb*^{-/-} mice also produced increased LCN-2 compared with uninfected C57Bl/6 mice, suggesting a propensity to inflammation in this mouse strain (Supplementary Fig. 3b). These results suggest that tetrathionate is produced during *S. typhimurium* infection, even in the absence of Cybb.

Mass spectrometry confirmed these results, directly detecting tetrathionate in cecum extracts from *S. typhimurium* $\Delta ttrR$ -infected

C57Bl/6 and all *cybb*^{-/-} mice, with infected mice showing significantly higher tetrathionate levels than uninfected ones ($P < 0.0001$ and $P = 0.002$ for C57Bl/6 and *cybb*^{-/-} mice, respectively) (Fig. 2c). We detected ~1 nanomole of tetrathionate from each inflamed mouse (Fig. 2c), translating to low micromolar concentrations if diluted across the approximate volume of the cecum (assuming 0.1–0.5 cm³ cecum volume); this concentration is on the order of the *in vitro* EC₅₀ of our sensor (Fig. 1c). Together these data show that the threshold of PAS638 sensing *in vivo* is on the order of 1 μ M, and that phagocyte NADPH-oxidase-independent tetrathionate production can be detected in the gut by our engineered *E. coli* strain. In contrast to previous reports we identified tetrathionate in *cybb*^{-/-} mice using the *S. typhimurium* $\Delta ttrR$ colitis model, both non-invasively by PAS638 response and by mass spectrometry detection¹⁴. These findings could foreseeably derive from sample measurement or microbiota differences between the studies.

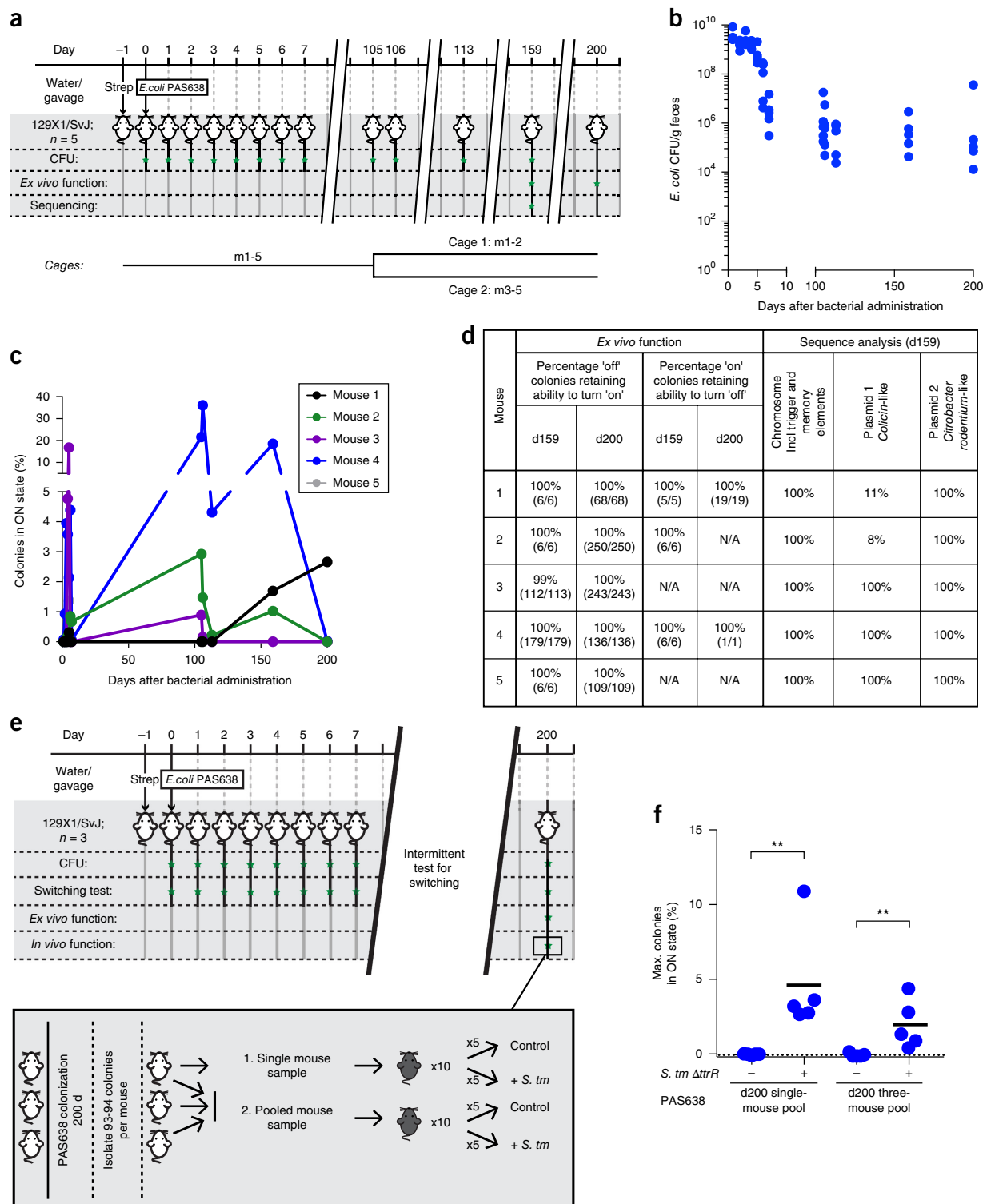


Figure 3 PAS638 does not accrue mutations in synthetic elements over long periods. **(a)** 129X1/SvJ mice were colonized with PAS638 for a 200-d period, >1,600 bacterial generations. Green star: analysis on fecal sample performed. Mice were housed together for days 1–105, and then separated into two cages. **(b)** PAS638 titers remained detectable after establishment in the streptomycin-treated gut, without further antibiotic selection. **(c)** Function was evident by switching at time points throughout the 200-d experiment. **(d)** Ex vivo functional tests and next-generation sequencing analysis of PAS638 colonies following 159 and 200 d of colonization confirmed that synthetic circuits did not mutate in any way over this period. For sequencing, result shown is percentage of non-mutated sequences. Only one mutational insertion (7879(A)₉₋₁₀) in the colicin-like plasmid was identified in two cohoused mice, m1 and m2. N/A, not available. **(e)** In vivo function was further confirmed through administration of PAS638 and *S. typhimurium* Δ trR to C57Bl/6 mice ($n = 5$ per group), using PAS638 colonies isolated after colonization of three separate 129X1/SvJ mice for 200 d. Pooled colonies from a single mouse (94 colonies), or all three mice (280 colonies) were tested. **(f)** Infection-specific PAS638 switching response confirmed functionality was retained in vivo. Graph shows maximum switching percentage measured 3–5 d after infection; means are marked. ** $P = 0.008$ using a two-tailed Mann–Whitney test of each experiment separately.

Increased ROS levels are also associated with IBD in humans²³ and may be present in patients even during subclinical inflammation. Interleukin-10-deficient mice (IL10^{-/-}) have features of human IBD, including the effect of microbiota composition on disease progression²⁴. To test whether PAS638 could detect subclinical inflammation in this model, we colonized ~6 month-old, retired-breeder IL10^{-/-} mice with PAS638 *E. coli* (Fig. 2d). These mice do not have acute colitis because they have been raised in gnotobiotic and barrier SPF conditions. The engineered bacteria (≥ 3 measurements over ≥ 2 weeks) detected tetrathionate in 8/9 IL10^{-/-} mice, but not in separately reared, retired C57Bl/6 breeder controls (Fig. 2e). Measurement of fecal LCN-2 showed that this marker of inflammation was temporarily increased in IL10^{-/-} mice immediately after administration but reduced after a week (Supplementary Fig. 3c). Switching levels in IL10^{-/-} mice were therefore measured more than 1 week after bacterial administration, which means that the inflammation sensed was not caused by the process of administration. To confirm that PAS638 did not cause inflammation, we administered PAS638 by oral gavage without antibiotic pre-treatment into IL10^{-/-} mice. PAS638 successfully colonized (Fig. 2f) and detected tetrathionate in 2/10 mice (2 measurements over 9 d) (Supplementary Fig. 3d). LCN-2 levels did not increase, in contrast to streptomycin-treated IL10^{-/-} mice (Supplementary Fig. 3e), suggesting that streptomycin rather than PAS638 caused the previously observed post-administration LCN-2 increase. This means that PAS638 can detect elevated tetrathionate in a physiologically relevant subclinical inflammatory environment.

To evaluate PAS638 in different mouse backgrounds, we administered the bacteria by oral gavage to BALB/c, C57Bl/6 or 129X1/SvJ mice, after overnight provision of streptomycin in their drinking water to assist in colonization, and measured the response over 5–8 d (≥ 3 measurements) (Fig. 2g). PAS638 did not respond in BALB/c or C57Bl/6 mice; surprisingly, however, bacteria from a subset (~20–40%) of 129X1/SvJ mice showed elevated switching (Fig. 2h). PAS638 gavage in the absence of streptomycin pre-treatment, while producing successful colonization (Supplementary Fig. 3f), also showed similar switching results (Supplementary Fig. 3g). Interestingly, histology did not reveal consistent signs of inflammation (Supplementary Fig. 3h). However, the presence of memory-on-state PAS638 bacteria correlated with the onset of elevated LCN-2 levels in five mice that were tested daily for 7 d (Fig. 2i), despite absolute LCN-2 levels being orders of magnitude lower than those measured during *Salmonella* infection (Supplementary Fig. 2d). While a definitive cause for the inflammation remained unclear, the 129X1/SvJ strain has documented defects in macrophage recruitment to sites of inflammation^{25,26}. Detection of tetrathionate in the presence of fluctuating and low-level inflammation that remained below histological detection further demonstrates the ability of PAS638 to detect a subclinical inflammatory environment.

Finally, we tested whether PAS638 could be used for long-term monitoring of tetrathionate. We used the PAS638-inducing environment of the 129X1/SvJ mouse to continually induce memory, thus allowing the fitness costs associated with both on and off states to be assessed. Five mice were colonized with PAS638 by oral gavage, after overnight provision of streptomycin in their drinking water, and maintained for 200 d, which corresponds to >1,600 bacterial generations²⁷. We used intermittent fecal testing to analyze the presence and function of PAS638 (Fig. 3a). Throughout this experiment PAS638 remained colonized at detectable levels without continued antibiotic selection (Fig. 3b), and colonies in the memory-on state were detected at each time point (Fig. 3c). Remarkably, colonies that were in the memory-off state in fecal samples at day 159 and day 200 retained the

ability to respond to tetrathionate *ex vivo* (Fig. 3d). Similarly, colonies that were in the memory-on state in fecal samples retained an ability to turn off memory under repeated streaking on agar plates (Fig. 3d). Together these results indicate that PAS638 had not acquired mutations to prevent its correct function.

PAS638 can colonize the mouse gut and retain the ability to respond to inflammation *in vivo* for at least 6 months. Colonies that retained *ex vivo* function were pooled from either one or three mice in a repeat long-term experiment, after 200 d of colonization (Supplementary Fig. 4a). Bacteria from these colonies were administered to C57Bl/6 mice in the presence or absence of *S. typhimurium* Δ trrR (Fig. 3e). Blinded scoring of histopathology, weight loss and LCN-2 concentrations all indicated successful infection (Supplementary Fig. 4b–d). The post-colonization PAS638 showed elevated switching specifically in mice also infected with *S. typhimurium* Δ trrR (Fig. 3f), confirming the ability of the engineered bacteria to function *in vivo* after extended growth in the gut.

Whole genome sequencing confirmed circuit stability. To analyze whether mutations had accrued in PAS638 during colonization, at day 159 PAS638 colonies from five mice (Fig. 3a) were pooled at the individual mouse level, and these were compared to the ancestral PAS638 by whole genome sequencing. The sequencing depth that was achieved (average chromosomal fold-coverage of 80–152) can identify mutations that occur in more than ~10% of the population. The only unique mutation identified from the five mouse samples was a repeat expansion in an intergenic region of the *E. coli* NGF-1 colicin-like plasmid, which was detected in 89% and 92% of reads from two mice (Fig. 3d). No mutations or rearrangements were detected on the chromosome, including the synthetic gene elements, or the NGF-1 *Citrobacter rodentium*-like plasmid. Further, junction prediction indicated that the synthetic elements remained in the same genomic location in all samples. The detected mutation, (A)_{9→10} in an intergenic region, is not expected to affect the function of the bacteria in any way. Detection of a single mutant is consistent with the number expected from wild-type *E. coli* over the ~1,200 generations in the gut^{28,29}. The two mice carrying bacteria with the detected mutations were housed together, while other mice were separated at day 105 (Fig. 3a). Given this mutation spread and fixed among the cohoused mice, we are confident that other beneficial mutations would have been detected at the sequencing depth achieved. Together these findings indicate that these synthetic circuits place a sufficiently low burden on the bacteria that harboring them does not affect bacterial function during more than 6 months in the complex gut environment.

These long-term experiments were facilitated by the use of *E. coli* NGF-1, which has high colonization capacity (Fig. 3b)¹². Plus, colonization by this strain does not require pre-administration of antibiotics, which improves the physiological relevance of our animal models.

Our results confirm the association of increased tetrathionate concentrations with inflammation both in the presence and absence of pathogen infection. We detected low-level inflammation in uninfected IL10^{-/-} and 129X1/SvJ mice. Further, in at least one case the PAS638 response provided more consistent results over a multiple-day period than LCN-2 measurement (Fig. 2i) due to the memory capacity of the engineered bacterial strain.

In conclusion, we show that synthetic bacterial devices can colonize the complex host mammalian gut and be used to monitor and analyze the course of a disease over an extended timeframe.

METHODS

Methods, including statements of data availability and any associated accession codes and references, are available in the [online version of the paper](#).

Note: Any Supplementary Information and Source Data files are available in the online version of the paper.

ACKNOWLEDGMENTS

We thank A. Graveline and L. Bry for discussions and assistance with mouse experiments and A. Verdegaaal for experimental assistance. *S. typhimurium* TT22470 was a gift from J. Roth. We thank Dana-Farber/Harvard Cancer Center in Boston for the use of the Rodent Histopathology Core, which provided histology preparation service. Dana-Farber/Harvard Cancer Center is supported in part by a NCI Cancer Center Support Grant # NIH 5 P30 CA06516. D.T.R. was supported by a Human Frontier Science Program Long-Term Fellowship and an NHMRC/RG Menzies Early Career Fellowship from the Menzies Foundation through the Australian National Health and Medical Research Council. T.W.G. was supported by a Leopoldina Research Fellowship (LPDS 2014-05) from the German National Academy of Sciences Leopoldina. The research was funded by Defense Advanced Research Projects Agency Grant HR0011-15-C-0094 (P.A.S.) and the Wyss Institute for Biologically Inspired Engineering.

AUTHOR CONTRIBUTIONS

D.T.R., T.W.G., M.B., S.J.K., G.K.G., J.C.W. and P.A.S. designed experiments. D.T.R. and M.J.N. performed and analyzed *in vitro* characterization. D.T.R. performed and analyzed all mouse experiments. T.W.G. performed and analyzed tetrathionate mass spectrometry. M.B. performed and analyzed whole genome sequencing. S.J.K. and J.W.K. generated strains and collected preliminary data for the study. R.T.B. performed all histology scoring. D.T.R. and P.A.S. wrote the manuscript.

COMPETING FINANCIAL INTERESTS

The authors declare no competing financial interests.

Reprints and permissions information is available online at <http://www.nature.com/reprints/index.html>. Publisher's note: Springer Nature remains neutral with regard to jurisdictional claims in published maps and institutional affiliations.

- Mimee, M., Citorik, R.J. & Lu, T.K. Microbiome therapeutics - advances and challenges. *Adv. Drug Deliv. Rev.* **105** Pt A, 44–54 (2016).
- Clairmont, C. *et al.* Biodistribution and genetic stability of the novel antitumor agent VNP20009, a genetically modified strain of *Salmonella typhimurium*. *J. Infect. Dis.* **181**, 1996–2002 (2000).
- Ceroni, F., Algar, R., Stan, G.-B. & Ellis, T. Quantifying cellular capacity identifies gene expression designs with reduced burden. *Nat. Methods* **12**, 415–418 (2015).
- Sleight, S.C. & Sauro, H.M. Visualization of evolutionary stability dynamics and competitive fitness of *Escherichia coli* engineered with randomized multigene circuits. *ACS Synth. Biol.* **2**, 519–528 (2013).
- Sleight, S.C., Bartley, B.A., Lieviant, J.A. & Sauro, H.M. Designing and engineering evolutionary robust genetic circuits. *J. Biol. Eng.* **4**, 12 (2010).
- Moser, F. *et al.* Genetic circuit performance under conditions relevant for industrial bioreactors. *ACS Synth. Biol.* **1**, 555–564 (2012).
- Gorochowski, T.E., van den Berg, E., Kerkman, R., Roubos, J.A. & Bovenberg, R.A.L. Using synthetic biological parts and microreactors to explore the protein expression characteristics of *Escherichia coli*. *ACS Synth. Biol.* **3**, 129–139 (2014).
- Gardner, T.S., Cantor, C.R. & Collins, J.J. Construction of a genetic toggle switch in *Escherichia coli*. *Nature* **403**, 339–342 (2000).
- Archer, E.J., Robinson, A.B. & Süel, G.M. Engineered *E. coli* that detect and respond to gut inflammation through nitric oxide sensing. *ACS Synth. Biol.* **1**, 451–457 (2012).
- Yang, L. *et al.* Permanent genetic memory with >1-byte capacity. *Nat. Methods* **11**, 1261–1266 (2014).
- Farzadfard, F. & Lu, T.K. Synthetic biology. Genomically encoded analog memory with precise *in vivo* DNA writing in living cell populations. *Science* **346**, 1256272 (2014).
- Kotula, J.W. *et al.* Programmable bacteria detect and record an environmental signal in the mammalian gut. *Proc. Natl. Acad. Sci. USA* **111**, 4838–4843 (2014).
- Mimee, M., Tucker, A.C., Voigt, C.A. & Lu, T.K. Programming a Human Commensal Bacterium, *Bacteroides thetaiotaomicron*, to Sense and Respond to Stimuli in the Murine Gut Microbiota. *Cell Syst.* **1**, 62–71 (2015).
- Winter, S.E. *et al.* Gut inflammation provides a respiratory electron acceptor for *Salmonella*. *Nature* **467**, 426–429 (2010).
- Kamdar, K. *et al.* Genetic and Metabolic Signals during Acute Enteric Bacterial Infection Alter the Microbiota and Drive Progression to Chronic Inflammatory Disease. *Cell Host Microbe* **19**, 21–31 (2016).
- Hensel, M., Hinsley, A.P., Nikolaus, T., Sawers, G. & Berks, B.C. The genetic basis of tetrathionate respiration in *Salmonella typhimurium*. *Mol. Microbiol.* **32**, 275–287 (1999).
- Winter, S.E., Lopez, C.A. & Bäuml, A.J. The dynamics of gut-associated microbial communities during inflammation. *EMBO Rep.* **14**, 319–327 (2013).
- Price-Carter, M., Tingey, J., Bobik, T.A. & Roth, J.R. The alternative electron acceptor tetrathionate supports B12-dependent anaerobic growth of *Salmonella enterica* serovar typhimurium on ethanolamine or 1,2-propanediol. *J. Bacteriol.* **183**, 2463–2475 (2001).
- Liu, Y.-W., Denkmann, K., Kosciow, K., Dahl, C. & Kelly, D.J. Tetrathionate stimulated growth of *Campylobacter jejuni* identifies a new type of bi-functional tetrathionate reductase (TsdA) that is widely distributed in bacteria. *Mol. Microbiol.* **88**, 173–188 (2013).
- Rooks, M.G. *et al.* Gut microbiome composition and function in experimental colitis during active disease and treatment-induced remission. *ISME J.* **8**, 1403–1417 (2014).
- Barthel, M. *et al.* Pretreatment of mice with streptomycin provides a *Salmonella enterica* serovar Typhimurium colitis model that allows analysis of both pathogen and host. *Infect. Immun.* **71**, 2839–2858 (2003).
- Chassaing, B. *et al.* Fecal lipocalin 2, a sensitive and broadly dynamic non-invasive biomarker for intestinal inflammation. *PLoS One* **7**, e44328 (2012).
- Simmonds, N.J. & Rampton, D.S. Inflammatory bowel disease--a radical view. *Gut* **34**, 865–868 (1993).
- Keubler, L.M., Buettner, M., Häger, C. & Bleich, A. A multihit model: colitis lessons from the interleukin-10-deficient mouse. *Inflamm. Bowel Dis.* **21**, 1967–1975 (2015).
- White, P., Liebhaber, S.A. & Cooke, N.E. 129X1/SvJ mouse strain has a novel defect in inflammatory cell recruitment. *J. Immunol.* **168**, 869–874 (2002).
- Hoover-Plow, J.L. *et al.* Strain and model dependent differences in inflammatory cell recruitment in mice. *Inflamm. Res.* **57**, 457–463 (2008).
- Myhrvold, C., Kotula, J.W., Hicks, W.M., Conway, N.J. & Silver, P.A. A distributed cell division counter reveals growth dynamics in the gut microbiota. *Nat. Commun.* **6**, 10039 (2015).
- Drake, J.W., Charlesworth, B., Charlesworth, D. & Crow, J.F. Rates of spontaneous mutation. *Genetics* **148**, 1667–1686 (1998).
- Lee, H., Popodi, E., Tang, H. & Foster, P.L. Rate and molecular spectrum of spontaneous mutations in the bacterium *Escherichia coli* as determined by whole-genome sequencing. *Proc. Natl. Acad. Sci. USA* **109**, E2774–E2783 (2012).

ONLINE METHODS

Strain construction. Details of strains constructed for this study are provided (Supplementary Table 1). All synthetic constructs were integrated chromosomally in the mouse commensal *Escherichia coli* NGF-1 strain¹² or *Salmonella typhimurium* 14028s.

The lambda-derived CI/Cro memory element was originally inserted between the *mhpR* and *lacZ* loci of *E. coli* TB10³⁰ and transferred to *E. coli* NGF-1 by P1vir transduction³¹, as previously described¹². Similarly, streptomycin resistance, conferred by a *rpsL* lys42arg mutation was previously generated and transferred from *E. coli* MG1655 to *E. coli* NGF-1 by P1vir transduction¹². The tetrathionate responsive trigger circuit, consisting of *ttrR*, *ttrS* genes and the P_{ttrBCA} promoter was amplified directly from *S. typhimurium* LT2. Overlap PCR was used to append the *cro* gene downstream of P_{ttrBCA} and add ~36-bp flanks for insertion into the *araB-araC* locus of *E. coli* TB10. The primer sets used were as follows: set 1: FW: ttatggataaaatgctatggcatagcaaaagt-gtga, REV: accagaatagcaacaacgtatgagccatgatgtgacggaagatcacttcgcagaataaa; set 2: FW atttattctgcaagtgatctccgtcacatcatggctcaccatggttctgtattctggt, REV: ataattctcagggttatcggtgttccatattgactcccgtccacattgccaacaatga; and set 3: FW tcatgttggcaatgtggacgggagtgcaataggaacaacgcataaccctgaaagattat, REV: acggcagaagaatccacattgattattgacggcgttatgctgtttttttgtactcgggaaggg. The locus was ultimately transferred to *E. coli* NGF-1 by P1vir transduction.

S. typhimurium strains were derived from *S. typhimurium* 14028s. To confer tetracycline resistance to all *S. typhimurium* strains a zhj-1401::Tn10 construct from *S. typhimurium* LT2 SA2700 (Salmonella Genetic Stock Center) was transferred to both *S. typhimurium* strains used in this study by P22 transduction³². To prevent tetrathionate reduction capacity, a *ttrR* knockout TT22470¹⁸ construct was transferred to *S. typhimurium* by P22 transduction.

In vitro induction with tetrathionate. Tetrathionate-based memory was induced under *in vitro* conditions in either liquid culture or during growth on plates. For liquid culture induction, strains were back-diluted 1:1,000 from overnight culture in Super Optimal Broth with Catabolite repression (SOC) broth into pre-reduced anaerobic SOC broth and grown at 37 °C in an anaerobic chamber (Coy Lab Products) using 7% H₂/ 20% CO₂/63% N₂ culture gas. After 1 h, potassium tetrathionate (Sigma) dissolved in pre-reduced SOC media was added to cultures, and induction was undertaken at 37 °C in the anaerobic chamber for 4 h. Memory was assayed by plating and growth in aerobic conditions of serial dilutions of the bacteria on Luria broth (LB) + 300 µg/mL streptomycin sulfate (Sigma) + 60 µg/mL 5-bromo-4-chloro-3-indolyl b-D-galactopyranoside (X-gal) (Santa Cruz Biotechnology) agar plates. Switching levels were estimated through counting greater than 250 blue and white colonies unless otherwise noted. *In vitro* testing on solid plates involved plating on LB + 300 µg/mL streptomycin sulfate (Sigma) + 60 µg/mL X-gal (Santa Cruz Biosciences) + 10 mM sodium tetrathionate (Sigma) agar. Growth was maintained in anaerobic conditions for ~8–12 h using the GasPak system (BD Biosciences), followed by further growth in aerobic conditions to allow development of memory and the X-gal reporter.

In vivo testing of tetrathionate memory. The Harvard Medical School Animal Care and Use Committee approved all animal study protocols.

General analysis. For most experiments, female, BALB/c (Charles River), C57Bl/6 (Charles River/Jackson Laboratory), 129X1/SvJ (Jackson Laboratory), B6.129P2-*Il10*^{tm1Cgn/J} (Jackson Laboratory) or B6.129S-*Cybb*^{tm1Din/J} (Jackson Laboratory) mice of 8–12 weeks, including ~2 weeks acclimatization to our mouse facility, were administered PAS638 *E. coli* NGF-1 bacteria (1 × 10^{7.8} CFU/mouse) by oral gavage. Except where specifically stated this occurred following pre-treatment with USP-grade streptomycin sulfate (Gold Biotechnology; 0.5 g/L in drinking water or 20 mg per mouse by oral gavage). Bacteria were pelleted and resuspended at a dilution of ~1/10 from overnight culture in sterile PBS before gavage of 100 µL/ mouse.

Fecal samples were collected from mice under study and homogenized at 50 or 100 mg/mL in sterile PBS by vortexing in 1.5 mL Eppendorf tubes for ~5 min. Large debris was pelleted from homogenized feces by centrifugation at 200 r.p.m. (4g) for 20 min in a benchtop centrifuge. Bacteria were cultured on agar plates following serial dilution of the resulting supernatant. Enumeration by colony counting and analysis of switching by comparison of blue (lac⁺, ON) and white (lac⁻, OFF) colony counts was achieved by plating on LB + 60 µg/mL

X-gal (Santa Cruz Biosciences) agar with 300 µg/mL streptomycin sulfate (Sigma), 34 µg/mL chloramphenicol (Sigma) or a combination of both drugs. All mice were pre-screened for the presence of resistant colonies in feces before bacterial administration. At least 250 colonies were counted per sample and where this was not possible results were excluded from switching quantification.

LCN-2 quantification was undertaken using the Mouse lipocalin-2/NGAL DuoSet ELISA kit (R&D Systems), using the manufacturer's recommended protocol. Samples for ELISA were prepared as previously described²², briefly, involving homogenization of 100 mg/mL fecal pellets in PBS + 0.1% Tween20 by vortexing for 20 min at 4 °C, followed by spinning at 12,000g for 10 min at 4 °C. Clear supernatant was diluted at least tenfold for quantification by ELISA. ELISA results were obtained on a Victor³V plate reader (PerkinElmer) with 450/8 nm and 540/8 nm absorbance filters. For analysis, absorbance corrected values were interpolated from a sigmoidal four parameter logistic standard curve using Prism 6 for Mac OS X software (GraphPad).

At the conclusion of the experiments, where required, mice were euthanized and dissected, their bowel removed and fixed whole in Bouin's fixative (Sigma). Fixed tissues were embedded in paraffin, sectioned and stained with hematoxylin and eosin. Scoring of severity of inflammation was undertaken on single longitudinal sections of whole gut in a blinded fashion by a trained rodent histologist (RTB).

At least four mice were used per experimental group, to which mice were assigned randomly where relevant. This sample size was estimated as a minimum based on its power to detect whether PAS638 had an overall detection capacity (a factor of both bacterial sensitivity and variability of mouse models) of ~47% with 95% confidence. These calculations treated the occurrence of above-threshold tetrathionate as a dichotomous variable given PAS638's low false-positive rate *in vitro* and in pilot *in vivo* experiments. For inflammation models determined to have higher variability or lower penetrance, larger sample sizes were used accordingly.

Streptomycin-treated *Salmonella colitis* model. The streptomycin-treated *Salmonella colitis* model was undertaken in C57Bl/6 (Charles River or Jackson Laboratories) and B6.129S-*Cybb*^{tm1Din} (Jackson Laboratories) mice, as previously described²¹. Briefly, mice were administered with 20 mg USP grade streptomycin sulfate (Gold Biotechnology) by oral gavage following 4 h nil per os (NPO). 24 h later, again following 4 h NPO, mice were administered bacterial strains, resuspended from overnight culture in phosphate buffered saline (Gibco), by oral gavage. Bacteria were administered at ~1 × 10^{7E. coli} and ~1 × 10^{8S. typhimurium} per mouse, as previously described²¹.

Selective plating for enumeration of *S. typhimurium* strains was achieved on M9 + 0.4% glucose + 30 µg/mL tetracycline (Sigma) agar. Enumeration and analysis of switching was achieved using plating on LB + 300 µg/mL streptomycin sulfate (Sigma) + 60 µg/mL X-gal (Santa Cruz Biosciences) agar.

IL10 knockout model. For initial experiments, male retired breeder mice (~6 months age) from an IL10^{-/-} background³³ were transferred to barrier SPF conditions, following growth under gnotobiotic conditions. The mice were colonized with a complex set of human commensal microbes, Gnotocomplex 2.0 (Supplementary Table 2), which is an expanded version of the Gnotocomplex designed to capture additional functionality and phylogenetic diversity³⁴. Control mice were male retired breeder mice (typically 6–8 months of age) from a C57Bl/6 background raised in SPF conditions (Charles River). Mice were administered PAS638 bacteria (~3 × 10⁷ per mouse) by oral gavage following USP streptomycin sulfate treatment (Gold Biotechnology; 0.5 g/L in drinking water). In mice where colonization was lower than 2.5 × 10⁴ CFU/g following gavage, streptomycin was re-administered within the first week following bacterial administration for up to 48 h to assist robust colonization.

Analysis of fecal samples was undertaken as described above. To avoid adverse influence of streptomycin and bacterial administration in IL10^{-/-} mice, which are sensitive to aberrant inflammatory responses (as evident from LCN-2 quantification in week 1 post administration (Supplementary Fig. 3c), blue-white colony screening was not undertaken in the week following administration. Results were generated from three to four fecal samples taken over the subsequent 2 weeks for control C57Bl/6 mice and ~1 month for IL10^{-/-} mice.

IL10^{-/-} studies were also undertaken in B6.129P2-*Il10*^{tm1Cgn/J} with administration of PAS638 occurring without streptomycin pre-treatment.

Tetrathionate quantification by mass spectrometry. Tetrathionate was quantified from extracts prepared from whole mouse cecum. Following dissection, the cecum was cut open and cecal contents were carefully removed from the underlying tissue and mucous layer. The mucosa was scraped with a blunt spatula and this was added to 500 μ L of water, which was additionally used to wash the cecal tissue by pipetting vigorously over the surface approximately ten times. The washed cecal tissue was then added to the same tube, and tissue and debris was removed by centrifugation at 10,000g for 10 min. Supernatants were then filter-sterilized using 13 mm 0.20 μ m, hydrophilic, PTFE syringe filters (Millex-LG) and frozen at -80°C before quantification.

High-performance liquid chromatography (HPLC)–tandem mass spectrometry (MS/MS) analysis of standards and extracts was carried out using an Agilent 1260 Infinity HPLC system equipped with an Agilent Eclipse Plus C18 column (100 \times 4.6 mm, particle size 3.5 μ m, flow rate: 0.5 mL/min, solvent A: 10 mM ammonium acetate in dd.H₂O, solvent B: acetonitrile, injection volume: 5 μ L) connected to an Agilent 6530 Accurate-Mass Q-TOF instrument. The following gradient was used (time/min, %B): 0, 0; 1, 0; 2, 95; 6, 95; 7, 0, 9, 0. The mass spectrometer was operated in negative mode and the autosampler was kept at 4 $^{\circ}\text{C}$. MS-fragmentation experiments were carried out using collision-induced dissociation (CID) fragmentation with nitrogen as the collision gas at 10 eV. By comparing fragmentation patterns of standards and samples, tetrathionate could be unequivocally identified.

The following fragments could be detected: 224.8660 ([S₄O₆H]⁻, parent ion), 144.9078 ([S₃O₃H]⁻) and 80.9652 ([SO₃H]⁻) (Supplementary Fig. 5).

To quantitate tetrathionate levels in extracts, a standard curve was recorded using freshly prepared sodium tetrathionate (Sigma) standards in distilled water (0.0001, 0.001, 0.01, 0.1 and 1 mM). Samples were kept on ice or at 4 $^{\circ}\text{C}$. After HPLC-MS/MS analysis, extracted ion chromatogram (EIC) peaks (224.84–224.88 Da) were automatically integrated using the MassHunter Workstation Software (version: B.07.00). A log-log plot of peak area versus tetrathionate concentration was used to generate a linear fit.

Whole genome sequencing and analysis. Bacterial samples were selected by plating from feces, as described above, on LB + 300 μ g/mL streptomycin sulfate (Sigma) + 60 μ g/mL X-gal (Santa Cruz Biosciences) agar. Colonies were scraped from plates, resuspended, and prepared for sequencing as a pool using a small-volume modification of the Illumina Nextera XP kit, as described previously³⁵. Sequencing was performed on the Illumina Miseq platform, using paired-end 50-bp reads. Raw sequence reads are available with links to NCBI BioProject accession number PRJNA380756.

Alignment and base calling of the ancestral sample was done via BreSeq³⁶ using default options, aligning to *E. coli* NGF-1 (NCBI references

NZ_CP016007.1, NZ_CP016008.1 and NZ_CP016009.1) and *E. coli* MG1655 (NCBI reference NC_000913.3) for sequences flanking engineered elements, which were cloned in *E. coli* MG1655 and transferred to the strain by P1 transduction. Breseq's gdttools package was used to modify the ancestral GenBank file to eliminate mutations in the ancestral strain. We then ran breseq at high sensitivity (settings-consensus-minimum-coverage-each-strand 3-consensus-frequency-cutoff 0.1) to call mutations in the passaged strains. Genomic coverage is as reported by breseq. As the number of reads at any given point is high, the chance of not seeing a mutation that occurs at $x\%$ of the population in at least k reads can be computed directly via Poisson approximation, i.e.,

$$1 - \sum_0^{k-1} \frac{k-1}{k!} 10^k e^{-10},$$

so for the case of a mutation in 10% of the population, at 100 \times coverage, there is a 99% chance it will appear in at least three independent reads.

Statistical analyses. All statistical analyses were undertaken in Prism 6 or 7 for Mac OS X (GraphPad). Details of individual tests and resulting P -values are included in figure legends and text where appropriate.

Data availability. Sequence reads are available at NCBI SRA (BioSample accession numbers SAMN06671873–SAMN06671878) linking to BioProject PRJNA380756.

E. coli NGF-1 assemblies for chromosome and plasmids are available with NCBI references NZ_CP016007.1, NZ_CP016008.1 and NZ_CP016009.1.

30. Datsenko, K.A. & Wanner, B.L. One-step inactivation of chromosomal genes in *Escherichia coli* K-12 using PCR products. *Proc. Natl. Acad. Sci. USA* **97**, 6640–6645 (2000).
31. Miller, J.H. *Experiments in Molecular Genetics* (Cold Spring Harbor Laboratory, 1972).
32. Davis, R.W., Botstein, D. & Roth, J.R. *A Manual for Genetic Engineering: Advanced Bacterial Genetics* (Cold Spring Harbor Laboratory, 1980).
33. Devkota, S. *et al.* Dietary-fat-induced taurocholic acid promotes pathobiont expansion and colitis in *Il10^{-/-}* mice. *Nature* **487**, 104–108 (2012).
34. Bucci, V. *et al.* MDSINE: Microbial Dynamical Systems Inference Engine for microbiome time-series analyses. *Genome Biol.* **17**, 121 (2016).
35. Baym, M. *et al.* Inexpensive multiplexed library preparation for megabase-sized genomes. *PLoS One* **10**, e0128036 (2015).
36. Deatherage, D.E. & Barrick, J.E. Identification of mutations in laboratory-evolved microbes from next-generation sequencing data using breseq. *Methods Mol. Biol.* **1151**, 165–188 (2014).